

Full Length Article

# A unified mechanism for oxidative coupling and partial oxidation of methane

Yves Simon<sup>\*</sup>, Paul-Marie Marquaire

Université de Lorraine, CNRS-Laboratoire Réactions et Génie des Procédés (UMR7274), ENSIC, 1 rue Grandville, BP 20451, F-54001 Nancy Cedex, France



## ARTICLE INFO

## Keywords:

Methane  
Kinetic mechanism  
Partial oxidation  
Oxidative coupling  
La<sub>2</sub>O<sub>3</sub>

## ABSTRACT

The oxidative coupling (OCM) and the partial catalytic oxidation (POM) of methane as well as the homogeneous oxidation of methane (HOM) differ only in the ratio CH<sub>4</sub>/O<sub>2</sub> used and of course in the use of a catalyst. It can therefore be considered that their overall reaction mechanism should be the same with elementary reactions of varying importance depending on the type of oxidation reaction studied. We have therefore tried to represent the results obtained during the experimental study of OCM and POM over La<sub>2</sub>O<sub>3</sub> and that of the oxidation of methane in gas phase from a single mechanism. At high temperature, OCM and POM are catalytic reactions but their reaction mechanisms are very complex because the surface reactions are coupled to reactions in gas phase by the intermediary of radicals, so both homogeneous and heterogeneous mechanisms occur at the same time. In this work, the development and the validation of a hetero-homogeneous mechanism is proposed for the three reactions. This mechanism is based on elementary steps at the catalyst surface and elementary steps in gas phase for a large range of temperature (973 K–1173 K) and residence time (0.7 s–5.5 s).

## 1. Introduction

Fluctuating prices of fossil fuel and discovery of new natural gas deposits are increasing interest in the upgrading of methane to value-added products. To date, the world reserve of natural gas is estimated about 198.8 trillion cubic meters [1] with steadily increasing in the future. Furthermore, over the past decade, increased production of shale gas has stimulated renewed interest to converting methane into valuable chemicals or liquid fuels.

The oxidative coupling of methane (OCM), first proposed by Keller and Bhasin [2] in 1982, is a direct method of converting methane into higher hydrocarbons especially ethylene. Ethylene is a critical intermediate in the petrochemical industry which is currently produced by steam cracking of hydrocarbon, mainly ethane. It is a highly endothermic reaction that occurs at high-temperature. Unlike steam cracking, the oxidative coupling of methane is exothermic and allows the direct conversion of methane into ethylene at a lower energy cost compared to current indirect industrial processes. During the 1990s, many studies were devoted to the OCM reaction. These studies showed that the yield of the reaction was not really compatible with an industrial application. However, in the last few years, the interest in the OCM reaction has increased because catalysts with higher activity and

selectivity have been found. Indeed, with oxides as La<sub>2</sub>O<sub>3</sub> acceptable reaction performances have been reached [3].

Another way of methane valorisation is the catalytic partial oxidation (POM). The catalytic partial oxidation of methane is an alternative to steam reforming [4,5] for synthesis gas (CO + H<sub>2</sub>) production. One advantage of POM is the production of syngas [6–8] with a H<sub>2</sub>/CO ratio ideal for a subsequent Fischer–Tropsch synthesis. In contrast to steam reforming, the partial oxidation is an exothermic reaction and therefore requires a smaller amount of heat energy. Furthermore, POM has a good dynamic response time and could therefore be used as an on-board hydrogen generator for fuel cells.

OCM and POM are catalytic reactions at high temperatures. Their reaction mechanisms are very complex because the surface reactions are coupled to reactions in gas phase by the intermediary of radicals [9–17], so both homogeneous and heterogeneous mechanisms occur at the same time. Indeed, the general oxidation mechanism includes two sub-mechanisms, one that is related to gas-phase and another that contains the catalytic reactions. Obviously, the homogeneous oxidation of methane (HOM) requires only the gas-phase mechanism. The modelling of the reaction by a detailed mechanism (composed of elementary steps describing the reaction as it occurs at the molecular level) has a lot of advantages. The mechanism and the kinetic analysis results allow a better understanding of the reaction. Indeed, based on this analysis, the

<sup>\*</sup> Corresponding author.

E-mail address: [yves.simon@univ-lorraine.fr](mailto:yves.simon@univ-lorraine.fr) (Y. Simon).

<https://doi.org/10.1016/j.fuel.2021.120683>

Received 11 September 2020; Received in revised form 27 December 2020; Accepted 14 March 2021

Available online 11 April 2021

0016-2361/© 2021 Elsevier Ltd. All rights reserved.

Nomenclature			
$k_i$	Rate constant for elementary step $i$	$\neq$	in relation with the activated complex
$A$	Arrhenius preexponential factor	$m$	molecule mass (kg)
$E$	Activation energy ( $\text{cal}\cdot\text{mol}^{-1}$ )	$M$	molar mass ( $\text{g}\cdot\text{mol}^{-1}$ )
$T$	temperature (K)	$s$	spin quantum number
$k_B$	Boltzmann constant, $1.381 \cdot 10^{-23} \text{ J}\cdot\text{K}^{-1}$	$\sigma_{\text{ext}}$	external symmetry number
$h$	Planck constant, $6.6262 \cdot 10^{-34} \text{ J}\cdot\text{s}$ .	$\sigma_{\text{int}}$	internal symmetry number
$N$	Avogadro number, $6.022 \cdot 10^{23}$	$I$	moment of inertia ( $\text{amu}\cdot\text{Å}^2$ or $\text{kg}\cdot\text{m}^2$ )
$Q_i$	total partition function for species $i$ ( $\text{m}^{-3}$ )	$I_{\text{red}}$	reduced moment of inertia ( $\text{amu}\cdot\text{Å}^2$ )
$Q_{\text{iv}}$	vibrational partition function for species $i$	$\omega$	frequency of vibration ( $\text{cm}^{-1}$ )
$Q_{\text{ir}}$	rotational partition function for species $i$	$D$	product of the moments of inertia ( $\text{amu}^3\cdot\text{Å}^6$ or $\text{kg}^3\cdot\text{m}^6$ )
$Q_{\text{it}}$	translational partition function for species $i$ ( $\text{m}^{-3}$ )	$\Delta H_{\text{ads},i}$	heat of adsorption for species $i$ ( $\text{cal}\cdot\text{mol}^{-1}$ )
$Q_{\text{ie}}$	electronic partition function for species $i$	$x_n$	molar fraction for species $n$
		$S_{i,n}$	sensibility coefficient of reactions $i$ for species $n$

reaction pathways, the importance of heterogeneous and homogeneous reactions and the limitative steps can be identified. Since 1982, the literature concerning the study of hetero-homogeneous reactions has been abundant [18,19]. However, there are few detailed mechanisms and much less kinetic data of surface reactions that were published.

The OCM and POM reactions differ only in the ratio  $\text{CH}_4/\text{O}_2$  used, so their overall reaction mechanism should be the same. We have therefore tried to represent the results obtained during the experimental study of OCM and POM over  $\text{La}_2\text{O}_3$  and that of the oxidation of methane in gas phase [20–23] from a single mechanism. The development and the validation of a hetero-homogeneous mechanism is proposed for the three reactions, based on elementary steps at the catalyst surface and on a homogeneous mechanism in gas phase for a large range of temperature and residence time. The experimental study was carried out in a perfectly stirred reactor in presence of lanthanum oxide. The

simulations were done by using the Chemkin® software packages.

## 2. Experimental section

The experimental setup was already described in previous articles [21,23].

The reactor developed for the investigation of hetero-homogeneous reactions [24,25] is a continuous stirred tank reactor (CSTR) presented in Fig. 1. It consists of two parts: an important well-stirred gas-phase volume ( $110 \text{ cm}^3$ ) in contact with catalysts pellets laid on a removable cylindrical support. Four Thermocoax resistance wires that are in contact with the wall are used for heating the reactor. Before entering the reactor, the reactant mixture is preheated. The temperature of the first preheating part is  $100 \text{ °C}$  lower than the reactor temperature while the temperature of the second preheating part equals the one of

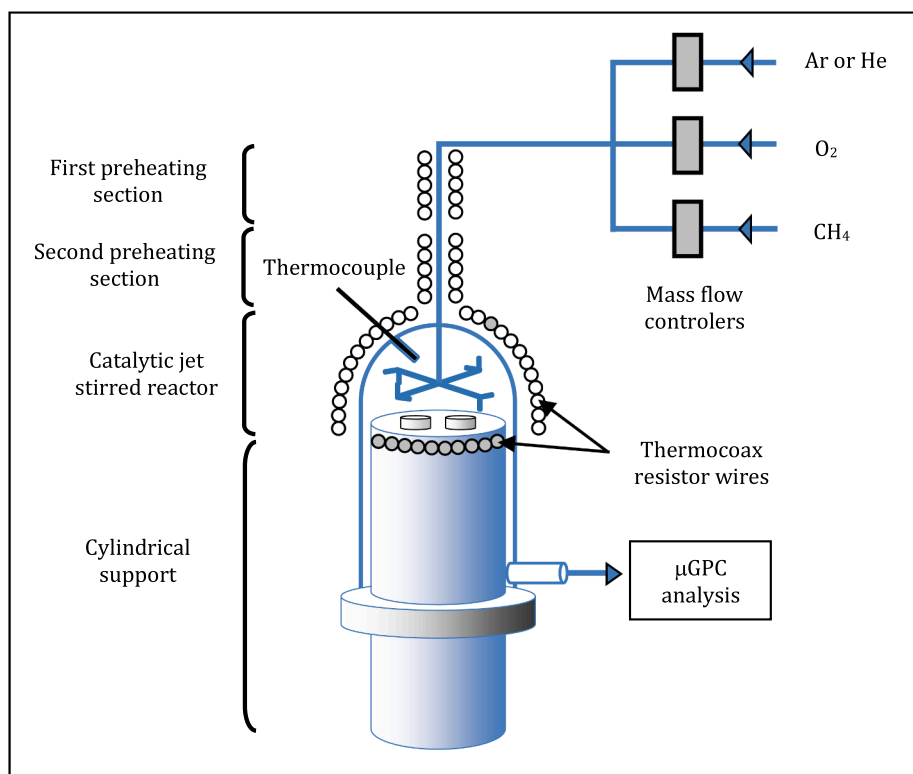


Fig. 1. Schematic representation of the catalytic jet-stirred reactor.

the reactor. The temperature of the gas phase is measured thanks to a thermocouple located inside a quartz finger at the middle of the free volume.

The catalyst used was Lanthanum oxide. The powder of  $\text{La}_2\text{O}_3$  was pelleted at a pressure of 20 kN into a cylindrical shape thanks to an electromechanical press Instron 5569. The pellets are 12 mm wide (diameter) and 1 mm thick. In order to facilitate the desorption of water and also to decompose the carbonates present on the surface of the pellets, the  $\text{La}_2\text{O}_3$  powder was heated for 8 h at a temperature of 900 °C. The BET surface areas are  $1.8 \text{ m}^2 \cdot \text{g}^{-1}$  for catalyst pellets used in OCM and  $5 \text{ m}^2 \cdot \text{g}^{-1}$  for pellets used in POM.

The outlet gases  $\text{H}_2$ ,  $\text{CO}$ ,  $\text{CH}_4$ ,  $\text{C}_2\text{H}_4$ ,  $\text{C}_2\text{H}_6$  and  $\text{CO}_2$  are analysed in line or off line by gas phase chromatography [21,23]. Several standard bottles, containing a gas mixture at different concentrations, externally calibrate the chromatograph. All data were collected at a steady state regime and each test was repeated at least three times to verify the stability and repeatability of the measurements.

The experimental conditions used for this study are:

- Temperatures between 973 K and 1173 K
- Outlet pressure fixed at 1 atm.
- Composition of the gas inlet with  $\text{CH}_4/\text{O}_2 = 5$  for OCM and  $\text{CH}_4/\text{O}_2 = 2$  for POM and HOM.

The reactants are highly diluted in argon or helium (94% in OCM and 84% in POM or HOM) to better control the reaction temperature and to avoid hot spots.

### 3. Kinetic modeling

#### 3.1. Homogeneous mechanism

The mechanism used for simulation includes a heterogeneous part and a homogeneous one. The homogeneous part is described by a set of over 450 elementary reactions. Due to its size, the mechanism cannot be fully presented here; we give only the most significant reactions in Table 1.

The homogeneous mechanism takes into account all elementary reactions between molecules and radicals including less than three carbon atoms. This gas-phase mechanism is well known and has been confirmed by a vast amount of experimental data for different hydrocarbon reactions for the homogeneous oxidation of methane [20,23,26].

This mechanism was generated by EXGAS software [27]. In the present work, this mechanism is used in combination with a heterogeneous mechanism for the simulation of the catalytic oxidation of methane reactions.

#### 3.2. Heterogeneous mechanism

##### 3.2.1. Description of the mechanism

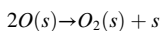
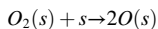
The development of the heterogeneous mechanism takes into account the results from mechanistic studies reported in the literature [28–37]. Despite the many studies carried out on this subject, the exact nature of the active sites on  $\text{La}_2\text{O}_3$  remains unclear. Yang et al. suggested that  $\text{O}^{2-}$  ions could be the active site for methane activation [38]. On the other hand for Hutchings et al. [39], the formation of  $\text{CH}_3$  radicals is due to the  $\text{O}^-$  ions while  $\text{O}_2^{2-}$  lead to the formation of  $\text{CH}_2$  radicals. Lacombe et al. [40] have identified various active sites on the surface of lanthanum oxide: a basic site associated with an anionic vacancy which would be responsible for the dissociation of gaseous oxygen into atomic species and an unsaturated site on which methyl radical would react to be further oxidized into  $\text{CO}_2$ . In summary, there are at least two types of active sites on the  $\text{La}_2\text{O}_3$  surface [41].

**Table 1**

Adjusted kinetic parameters of most important homogeneous reactions in oxidation of methane.  $k = A(T) \exp(-E/RT)$ .

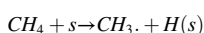
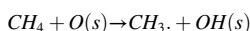
Reactions	A (mol, cm <sup>3</sup> , s)	n	E <sub>a</sub> (cal. mol <sup>-1</sup> )	
1	$\text{O}_2 + \text{H} = \text{OH} + \text{O}$	$1.5 \cdot 10^{14}$	0.0	14,810
2	$\text{O}_2 + \text{H} (+\text{M}) = \text{HO}_2 (+\text{M})$	$4.52 \cdot 10^{13}$	0.0	0.0
3	$\text{O}_2 + \text{CHO} = \text{CO} + \text{HO}_2$	$2.6 \cdot 10^{11}$	0.0	410
4	$\text{O}_2 + \text{CH}_3 = \text{CH}_3\text{O} + \text{O}$	$1.6 \cdot 10^{13}$	0.0	31,300
5	$\text{O}_2 + \text{HCHO} = \text{CHO} + \text{HO}_2$	$2.0 \cdot 10^{13}$	0.0	38,800
6	$\text{O}_2 + \text{CH}_3 = \text{HCHO} + \text{OH}$	$3.0 \cdot 10^{30}$	-4.69	36,600
7	$\text{O}_2 + \text{CH}_4 = \text{CH}_3 + \text{HO}_2$	$4.0 \cdot 10^{13}$	0.0	56,700
8	$\text{O}_2 + \text{C}_2\text{H}_5 = \text{C}_2\text{H}_4 + \text{HO}_2$	$8.4 \cdot 10^{11}$	0.0	3900
9	$\text{O}_2 + \text{C}_2\text{H}_3 = \text{HCHO} + \text{CHO}$	$4.5 \cdot 10^{16}$	-1.39	1000
10	$\text{O}_2 + \text{C}_2\text{H}_3 = \text{C}_2\text{H}_2 + \text{HO}_2$	$1.34 \cdot 10^6$	1.61	-400
11	$\text{O}_2 + \text{C}_2\text{H}_2 = 2 \text{CHO}$	$7.0 \cdot 10^8$	1.8	30,600
12	$\text{O} + \text{H}_2 = \text{OH} + \text{H}$	$5.1 \cdot 10^4$	2.67	6200
13	$\text{O} + \text{CH}_3 = \text{HCHO} + \text{H}$	$8.4 \cdot 10^{13}$	0.0	0
14	$\text{O} + \text{CH}_4 = \text{CH}_3 + \text{OH}$	$7.2 \cdot 10^8$	1.56	8400
15	$\text{O} + \text{C}_2\text{H}_6 = \text{C}_2\text{H}_5 + \text{OH}$	$1.0 \cdot 10^9$	1.5	5800
16	$\text{O} + \text{C}_2\text{H}_4 = \text{CH}_3 + \text{CHO}$	$8.1 \cdot 10^6$	1.88	200
17	$\text{O} + \text{C}_2\text{H}_4 = \text{HCHO} + \text{CH}_2$	$4.0 \cdot 10^5$	1.88	200
18	$\text{O} + \text{C}_2\text{H}_4 = \text{CH}_2\text{CO} + \text{H}_2$	$6.6 \cdot 10^5$	1.88	200
19	$\text{O} + \text{C}_2\text{H}_4 = \text{CH}_2\text{CHO} + \text{H}$	$4.7 \cdot 10^6$	1.88	200
20	$\text{O} + \text{C}_2\text{H}_4 = \text{OH} + \text{C}_2\text{H}_3$	$1.5 \cdot 10^7$	1.91	3700
21	$\text{O} + \text{HCHO} = \text{CHO} + \text{OH}$	$4.1 \cdot 10^{11}$	0.57	2700
22	$\text{OH} + \text{H}_2 = \text{H} + \text{H}_2\text{O}$	$1.0 \cdot 10^8$	1.6	3300
23	$\text{OH} + \text{CH}_3 (+\text{M}) = \text{CH}_3\text{OH} (+\text{M})$	$6.0 \cdot 10^{13}$	0.0	0
24	$\text{OH} + \text{CH}_4 = \text{CH}_3 + \text{H}_2\text{O}$	$1.6 \cdot 10^7$	1.83	2700
25	$\text{OH} + \text{CO} = \text{CO}_2 + \text{H}$	$6.3 \cdot 10^6$	1.5	-500
26	$\text{OH} + \text{HCHO} = \text{CHO} + \text{H}_2\text{O}$	$3.4 \cdot 10^9$	1.18	-400
27	$\text{OH} + \text{C}_2\text{H}_4 = \text{C}_2\text{H}_3 + \text{H}_2\text{O}$	$2.0 \cdot 10^{13}$	0.0	5900
28	$\text{OH} + \text{C}_2\text{H}_4 = \text{CH}_3 + \text{HCHO}$	$2.0 \cdot 10^{12}$	0.0	900
29	$\text{OH} + \text{C}_2\text{H}_6 = \text{C}_2\text{H}_5 + \text{H}_2\text{O}$	$7.2 \cdot 10^6$	2.0	900
30	$2 \text{HO}_2 = \text{H}_2\text{O}_2 + \text{O}_2$	$4.2 \cdot 10^{14}$	0.0	11,980
31	$\text{HO}_2 + \text{H} = 2 \text{OH}$	$1.7 \cdot 10^{14}$	0.0	900
32	$\text{HO}_2 + \text{CH}_3 = \text{CH}_3\text{O} + \text{OH}$	$1.8 \cdot 10^{13}$	0.0	0
33	$\text{HO}_2 + \text{CH}_4 = \text{CH}_3 + \text{H}_2\text{O}_2$	$9.0 \cdot 10^{12}$	0.0	24,600
34	$\text{HO}_2 + \text{CO} = \text{CO}_2 + \text{OH}$	$1.5 \cdot 10^{15}$	0.0	23,600
35	$\text{HO}_2 + \text{CHO} = \text{OH} + \text{H} + \text{CO}_2$	$3.0 \cdot 10^{13}$	0.0	0
36	$\text{HO}_2 + \text{HCHO} = \text{CHO} + \text{H}_2\text{O}_2$	$3.0 \cdot 10^{12}$	0.0	13,000
37	$\text{HO}_2 + \text{C}_2\text{H}_6 = \text{C}_2\text{H}_5 + \text{H}_2\text{O}_2$	$1.3 \cdot 10^{13}$	0.0	20,400
38	$2 \text{CH}_3 (+\text{M}) = \text{C}_2\text{H}_6 (+\text{M})$	$3.6 \cdot 10^{13}$	0.0	0.0
39	$2 \text{CH}_3 = \text{C}_2\text{H}_5 + \text{H}$	$3.0 \cdot 10^{13}$	0.0	13,500
40	$2\text{CH}_3 = \text{C}_2\text{H}_4 + \text{H}_2$	$2.1 \cdot 10^{14}$	0.0	19,300
41	$\text{CH}_3 + \text{H} (+\text{M}) = \text{CH}_4 (+\text{M})$	$1.7 \cdot 10^{14}$	0.0	0.0
42	$\text{CH}_3 + \text{HCHO} = \text{CHO} + \text{CH}_4$	$7.7 \cdot 10^8$	6.1	1970
43	$\text{CH}_4 + \text{H} = \text{CH}_3 + \text{H}_2$	$1.3 \cdot 10^4$	3.0	8000
44	$\text{C}_2\text{H}_2 + \text{H} (+\text{M}) = \text{C}_2\text{H}_3 (+\text{M})$	$8.4 \cdot 10^{12}$	0.0	2610
45	$\text{C}_2\text{H}_3 (+\text{M}) = \text{C}_2\text{H}_2 + \text{H}$	$2.0 \cdot 10^{14}$	0.0	39,800
46	$\text{C}_2\text{H}_4 (+\text{M}) = \text{C}_2\text{H}_2 + \text{H}_2 (+\text{M})$	$1.0 \cdot 10^{17}$	0.0	71,600
47	$\text{C}_2\text{H}_4 + \text{H} = \text{C}_2\text{H}_3 + \text{H}_2$	$5.1 \cdot 10^7$	1.93	12,900
48	$\text{C}_2\text{H}_4 + \text{CH}_3 = \text{CH}_4 + \text{C}_2\text{H}_3$	$6.3 \cdot 10^{11}$	0.0	1600
49	$\text{C}_2\text{H}_4 + \text{CH}_3 = \text{C}_3\text{H}_7$	$2.1 \cdot 10^{10}$	0.0	7350
50	$\text{C}_2\text{H}_5 (+\text{M}) = \text{C}_2\text{H}_4 + \text{H} (+\text{M})$	$8.2 \cdot 10^{13}$	0.0	40,000
51	$\text{C}_2\text{H}_6 (+\text{M}) = \text{C}_2\text{H}_4 + \text{H}_2 (+\text{M})$	$2.3 \cdot 10^{17}$	0.0	67,400
52	$\text{C}_2\text{H}_6 + \text{H} = \text{C}_2\text{H}_5 + \text{H}_2$	$1.4 \cdot 10^9$	1.5	7400
53	$\text{C}_2\text{H}_6 + \text{CH}_3 = \text{C}_2\text{H}_5 + \text{CH}_4$	$1.5 \cdot 10^7$	6.0	5800
54	$\text{C}_2\text{H}_6 (+\text{M}) = 2\text{CH}_3 (+\text{M})$	$1.8 \cdot 10^{21}$	-1.24	90,900
55	$\text{CHO} (+\text{M}) = \text{H} + \text{CO} (+\text{M})$	$1.6 \cdot 10^{14}$	0.0	15,700
56	$\text{CHO} + \text{CH}_3 = \text{CH}_4 + \text{CO}$	$1.2 \cdot 10^{14}$	0.0	0.0
58	$\text{HCHO} + \text{H} = \text{CHO} + \text{H}_2$	$1.3 \cdot 10^8$	1.62	3100
59	$\text{CH}_2\text{CO} (+\text{M}) = \text{CH}_2 + \text{CO} + (\text{M})$	$6.57 \cdot 10^{15}$	0.0	57,600
60	$\text{CH}_2\text{CO} + \text{H} = \text{CH}_3 + \text{CO}$	$1.8 \cdot 10^{13}$	0.0	3400
61	$\text{CH}_3\text{O}_2 = \text{HCHO} + \text{OH}$	$1.5 \cdot 10^{13}$	0.0	47,000
62	$\text{CH}_3\text{O}_2 + \text{CH}_4 = \text{CH}_3\text{O}_2\text{H} + \text{CH}_3$	$1.8 \cdot 10^{11}$	0.0	18,500
63	$\text{CH}_3\text{O}_2 + \text{CH}_3 = 2 \text{CH}_3\text{O}$	$5.0 \cdot 10^{12}$	0.0	-1400

In our mechanism, the two types of active sites considered are: a reduced site (s) and an oxygenated site O(s). Experimental studies of oxygen chemisorption [42] have shown that this reaction occurs with dissociation of a diatomic O<sub>2</sub> molecule to form two active atomic oxygen centres according to the following reaction:

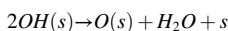
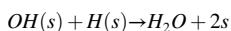
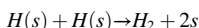


In these elementary reactions s represents a surface site and O(s) the atom O adsorbed on the surface of the La<sub>2</sub>O<sub>3</sub> crystal.

The heterogeneous mechanism was written systematically by considering the possible reactions between these two sites and the major reaction products and free radicals. These reactions were written according to the Eley-Rideal formalism involving the reactions between a gas phase molecule and an active site. For example, methane can react according to:



The hydroxylated sites and hydrogenated sites can react according to the Langmuir-Hinshelwood formalism leading to the formation of hydrogen and water via surface steps:



Finally, the heterogeneous mechanism is composed of 33 direct elementary steps involving 9 surface species (Table 2).

To carry out the simulations, it is necessary to calculate the kinetics

**Table 2**  
Kinetic parameters of surface reactions in oxidation of methane.

Réactions	A (mol, cm <sup>2</sup> , s)	E(cal.mol <sup>-1</sup> )
1 O <sub>2</sub> + s → O <sub>2</sub> (s)	1.8 10 <sup>7</sup>	1500
2 O <sub>2</sub> (s) → O <sub>2</sub> + s	2,3 10 <sup>12</sup>	45,000
3 O <sub>2</sub> (s) + s → 2O(s)	1.2 10 <sup>23</sup>	25,000
4 2O(s) → O <sub>2</sub> (s) + s	3.3 10 <sup>23</sup>	33,000
5 CH <sub>4</sub> + O(s) → CH <sub>3</sub> · + OH(s)	7.5 10 <sup>8</sup>	8840
6 C <sub>2</sub> H <sub>6</sub> + O(s) → C <sub>2</sub> H <sub>5</sub> · + OH(s)	9.5 10 <sup>9</sup>	3000
7 CO + O(s) → CO <sub>2</sub> + s	4.7 10 <sup>9</sup>	0
8 CO <sub>2</sub> + s → CO <sub>2</sub> (s)	6.2 10 <sup>8</sup>	0
9 CO <sub>2</sub> (s) → CO <sub>2</sub> + s	2.3 10 <sup>13</sup>	43,580
10 C <sub>2</sub> H <sub>4</sub> + O(s) → C <sub>2</sub> H <sub>3</sub> · + OH(s)	5.5 10 <sup>8</sup>	3000
11 C <sub>2</sub> H <sub>5</sub> · + O(s) → C <sub>2</sub> H <sub>4</sub> + OH(s)	5.5 10 <sup>7</sup>	0
12 C <sub>3</sub> H <sub>7</sub> · + O(s) → C <sub>3</sub> H <sub>6</sub> + OH(s)	6.1 10 <sup>7</sup>	0
13 2OH(s) → O(s) + H <sub>2</sub> O + s	1.3 10 <sup>23</sup>	2400
14 CH <sub>3</sub> · + O(s) → CH <sub>2</sub> · + OH(s)	1.9 10 <sup>9</sup>	2800
15 CH <sub>2</sub> · + O(s) → CH· + OH(s)	3.6 10 <sup>11</sup>	11,900
16 CH· + O(s) → C + OH(s)	8.9 10 <sup>8</sup>	4700
17 C + O(s) → CO + s	1.1 10 <sup>11</sup>	0
18 CH <sub>3</sub> · + O(s) → CH <sub>3</sub> O(s)	9.9 10 <sup>8</sup>	600
19 CH <sub>3</sub> O(s) + O(s) → HCHO + OH(s) + s	1.2 10 <sup>23</sup>	0
20 HCHO + O(s) → CHO· + OH(s)	3.4 10 <sup>7</sup>	3000
21 CHO· + O(s) → CO + OH(s)	6.9 10 <sup>7</sup>	410
22 C <sub>2</sub> H <sub>5</sub> · + O(s) → C <sub>2</sub> H <sub>5</sub> O(s)	1.0 10 <sup>9</sup>	600
23 C <sub>2</sub> H <sub>5</sub> O(s) + O(s) → CH <sub>3</sub> CHO + OH(s) + s	6.6 10 <sup>21</sup>	0
24 CH <sub>4</sub> + s → CH <sub>3</sub> · + H(s)	8.5 10 <sup>7</sup>	9850
25 C <sub>2</sub> H <sub>6</sub> + s → C <sub>2</sub> H <sub>5</sub> · + H(s)	9.8 10 <sup>7</sup>	5000
26 C <sub>2</sub> H <sub>4</sub> + s → C <sub>2</sub> H <sub>3</sub> · + H(s)	1.9 10 <sup>7</sup>	5000
27 H· + s → H(s)	9.6 10 <sup>12</sup>	0
28 OH(s) + H(s) → H <sub>2</sub> O + 2 s	1.0 10 <sup>24</sup>	0
29 H(s) + H(s) → H <sub>2</sub> + 2 s	1.3 10 <sup>23</sup>	0
30 H <sub>2</sub> + 2 s → 2H(s)	6.1 10 <sup>16</sup>	0
31 H <sub>2</sub> + O(s) → OH(s) + H·	1.0 10 <sup>10</sup>	0
32 C + O(s) → CO(s)	1.1 10 <sup>11</sup>	0
33 CO(s) + O(s) → CO <sub>2</sub> (s) + s	1.1 10 <sup>23</sup>	0

[s symbolizes surface site and (s) adsorbed species].

parameters of this heterogeneous mechanism. There are few models involving a detailed mechanism composed of elementary steps and with estimation of the kinetics parameters. We can quote for example Deutschmann [43], Sinev [44] and Gent University [45]. In our study, pre-exponential factor of elementary steps are calculated by methods derivate from Benson's techniques [46] whereas activation energies are chosen in first approximation by analogy with reactions in gas phase. Simulations were performed using the Chemkin® and Surface Chemkin® software packages in a CSTR reactor [47,48]. The simulations were performed by simultaneously compiling the homogeneous and the heterogeneous sub-mechanisms so that the possible coupling could be taken into account. It should be noted that these methods give only an approximation of the initial numerical value of parameters, usually unknown, which must be adjusted during the optimization from experimental results.

### 3.2.2. Pre-exponential factor

The pre-exponential factor is calculated by using partition functions of gas molecule and activated complex. For the following reaction:



where A is a gas molecule, B(s) a surface species and AB<sup>‡</sup> the activated complex, the pre-exponential factor is calculated by the following equation:

$$A = \frac{k_B T N q^\ddagger}{h q_A q_{B(s)}} \quad (1)$$

In Eq. (1), k<sub>B</sub> is the Boltzmann constant (1.38 10<sup>-23</sup> J.K<sup>-1</sup>), N the Avogadro constant (6.022 10<sup>23</sup> mol<sup>-1</sup>), T the temperature, h the Planck constant (6.6262 10<sup>-34</sup> J.s.) and q<sub>A</sub>, q<sub>B(s)</sub>, q<sup>‡</sup> are the partition functions of A, B(s) and the activated complex. The difference between the degrees of freedom of B(s) and AB<sup>‡</sup> is mainly due to the vibrations of the molecule A in the configuration of the activated complex. Indeed, B(s) and AB<sup>‡</sup> are adsorbed species and have no rotational or translational degrees of freedom. So, to simplify the calculation, we suppose that the difference between partition function of B(s) and AB<sup>‡</sup> is only due to the vibrational component of the activated complex q<sup>‡</sup><sub>v</sub>. Then the following expression is obtained:

$$A = \frac{k_B T N q_v^\ddagger}{h q_A} \quad (2)$$

The partition function of a molecule or a radical is the product of a translational partition function q<sub>t</sub>, an external rotational partition function q<sub>r</sub>, a vibrational partition function q<sub>v</sub> and an electronic partition function q<sub>e</sub>. These partition functions can be calculated by the Eq. (3).

$$q_t = \frac{(2\pi m k_B T)^{3/2}}{h^3}$$

$$q_r^{3D} = \frac{\pi^{1/2}}{\sigma_{\text{ext}}} \left( \frac{8\pi^2 k_B T}{h^2} \right)^{3/2} R^{1/2} \quad \text{or} \quad q_r^{2D} = \frac{8\pi^2 I k_B T}{\sigma_{\text{ext}} h^2} \quad (3)$$

$$q_v = \prod_i q_{v,i} \quad \text{and} \quad q_{v,i} = \frac{1}{1 - \exp\left(\frac{-1.44\omega_i}{T}\right)}$$

$$q_e = 2s + 1$$

In these equations, σ<sub>ext</sub> is the external symmetry number, m (kg) the mass of the atom, s the spin and ω<sub>i</sub> (cm<sup>-1</sup>) the frequency of the tabulated vibration.

The selection of the formula for calculating the rotational partition function depends on the molecule considered. A linear molecule only possesses two rotational degrees of freedom. The two moments of inertia about the two axes of rotation are equal to I (kg.m<sup>2</sup>). In this case, the rotational partition function is q<sub>r</sub><sup>2D</sup>. However, there are 3 rotational degrees of freedom in a non-linear molecule and the calculation of the

partition function  $q_r^{3D}$  use the product of the moments of inertia:  $D$  ( $\text{kg}^3 \cdot \text{m}^6$ ). For easier use, these formulas can be rewritten:

$$q_t = 1.88 \cdot 10^{26} (MT)^{3/2}$$

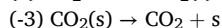
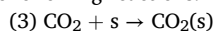
$$q_r^{3D} = 1.48 \cdot 10^{-2} \frac{D^{1/2} T^{3/2}}{\sigma_{\text{ext}}} \quad \text{or} \quad q_r^{2D} = 4.12 \cdot 10^{-2} \frac{IT}{\sigma_{\text{ext}}} \quad (4)$$

In the first expression the unit of  $q_t$  is  $\text{m}^{-3}$  and  $M$  is the molar mass ( $\text{g} \cdot \text{mol}^{-1}$ ). In the second expression, the unit of  $D$  is  $\text{amu}^3 \cdot \text{\AA}^6$  and that of  $I$  is  $\text{amu} \cdot \text{\AA}^2$ .

### 3.2.3. Activation energy

The activation energy is the most difficult parameter to calculate, especially for surface reactions, because it depends on the nature of the adsorption site. Since these values are generally intended to be optimized by simulation of the experimental results, two simple methods of estimation depending on the type of reaction involved are proposed. For the adsorption/desorption reactions, the activation energy is calculated from the experimental value of adsorption enthalpy obtained from the literature. The activation energy of the other elementary surface reactions can be assumed in first estimate to be the same as the equivalent gas-phase reaction.

For example, the  $\text{CO}_2$  adsorption – desorption can be represented by the following reactions:



The activation energy of the  $\text{CO}_2$  adsorption is low; so the activation energy of the step (3) is supposed to be equal to 0. The adsorption enthalpy of  $\text{CO}_2$  on the surface can be found in the literature; the adsorption enthalpy of  $\text{CO}_2$  on  $\text{La}_2\text{O}_3/\text{CaO}$  catalyst [49] is about:

$$-\Delta H_{\text{ads, CO}_2} = 44 \pm 7 \text{ kcal} \cdot \text{mol}^{-1} = E_{-3}$$

For the other types of surface reactions, the activation energy can be chosen, by analogy with gas phase reactions. The Eley-Rideal reaction of an ethane molecule with the surface of the catalyst:  $\text{C}_2\text{H}_6 + s \rightarrow \text{C}_2\text{H}_5 \cdot + \text{H}(s)$  may be represented by the following homogeneous reaction:  $\text{C}_2\text{H}_6 + \text{alkyl} \cdot \rightarrow \text{C}_2\text{H}_5 \cdot + \text{alkane}$

We can use, for example, the reaction:  $\text{C}_2\text{H}_6 + \text{CH}_3 \cdot \rightarrow \text{C}_2\text{H}_5 \cdot + \text{CH}_4$

The activation energy of this gas phase reaction [50] is:  $5800 \text{ cal} \cdot \text{mol}^{-1}$ . At a first approximation, this value for the activation energy of the surface reaction can be used. The activation energy depends on the catalyst surface and these activation energy values can only be considered as a starting point for the simulation. Finally, a hetero-homogeneous mechanism composed of many elementary steps and their kinetic constants ( $A$  and  $E$ ) was obtained.

### 3.3. Sensitivity analysis

For all the reactions studied, a flow consumption analysis or a sensitivity analysis can be realized to better understand the reaction and to find optimal conditions. To determine the most sensitive reactions involved in the mechanism, a sensitivity analysis was performed for each of the three reactions. The analysis was performed for major products. Figs. 2 and 3 show sensitivity analysis for surface reactions for OCM and POM. The first order sensitivity coefficient for species  $n$  and reaction  $i$  was defined according to:

$$S_{i,n} = \frac{k_i}{dk_i} \frac{dx_n}{x_n} \quad (5)$$

where  $k_i$  is the kinetic constant of reaction  $i$  and  $x_n$  is the molar fraction of species  $n$ . The higher the  $S_{i,n}$  coefficient is, the more sensitive against species  $n$  the reaction  $i$  is. Moreover, a positive sensitivity coefficient  $S_{i,n}$  means that an increase of the kinetic constant  $k_i$  leads to an increase of the concentration of species  $n$ . Some reactions have sensitivity coefficients lower than  $|0.01|$  and can be considered negligible. Table 3 shows the final surface mechanism in which only the most important elementary reactions are present. This simplified mechanism

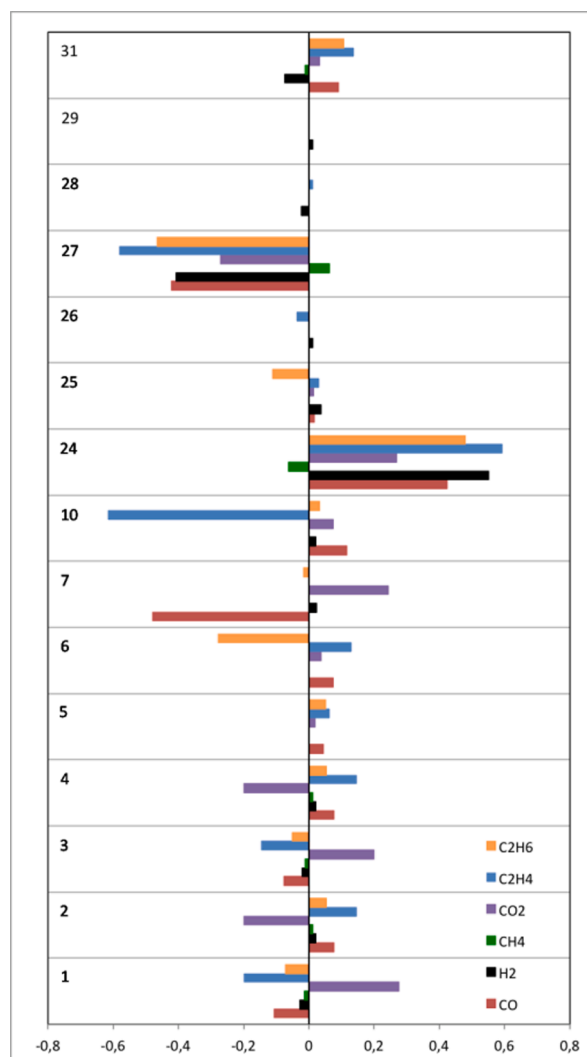


Fig. 2. Sensitivity analysis of surface reactions for POM at 1123 K.

consists of 17 elementary reactions and gives the same result as the complete mechanism with an error of less than 1%.

## 4. Results and discussion

For the three reactions of OCM, POM and HOM, the experimental curves of reactant consumption and product formation as a function of residence time were simulated. The kinetic parameters of the homogeneous reactions provide from literature [51–59] or are calculated by the Kingas [60] software (Table 1). The kinetic parameters of heterogeneous reactions are estimated using the methodology described here (Table 2) and modified to fit the model to the experimental results (Table 3). This unified hetero-homogeneous mechanism is used for the simulation of the three reactions.

### 4.1. Homogeneous oxidation of methane

Homogeneous oxidation of methane doesn't have a real industrial interest because of the stability of the methane molecule. However, the mechanism of this reaction is essential to represent the reactions of OCM and POM. Therefore, we have studied this reaction experimentally over a large temperature range (1083 K to 1148 K) in order to determine its reaction mechanism. Figs. 4–9 show the molar fraction of  $\text{CH}_4$ ,  $\text{C}_2\text{H}_4$ ,  $\text{C}_2\text{H}_6$ ,  $\text{CO}$ ,  $\text{CO}_2$  and  $\text{H}_2$  versus residence time. The ratio  $\text{CH}_4/\text{O}_2$  was fixed

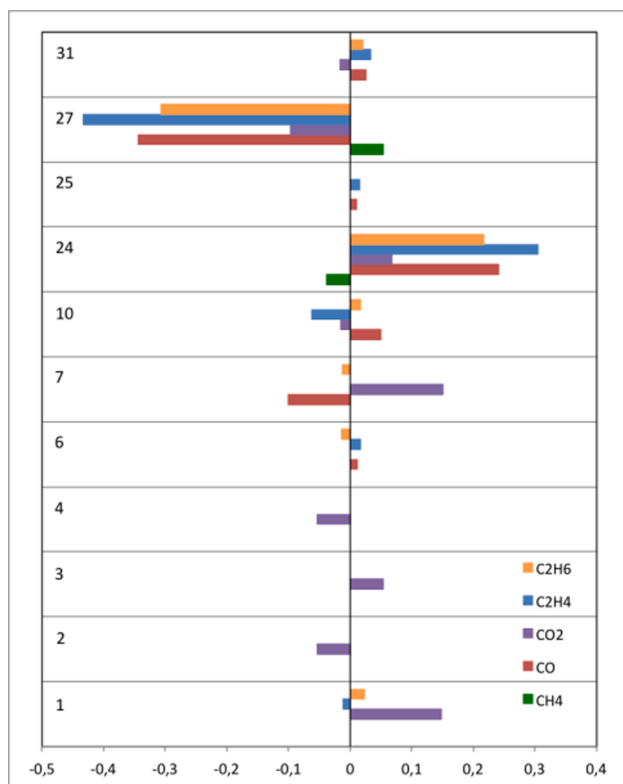


Fig. 3. Sensitivity analysis of surface reactions for OCM at 1173 K.

Table 3

Simplified surface mechanism of methane oxidation [s symbolizes surface site and (s) adsorbed species].

Réactions	$A_{\text{fitted}}$ (mol, cm <sup>2</sup> , s)	$E_{\text{fitted}}$ (cal.mol <sup>-1</sup> )
1 $O_2 + s \rightarrow O_2(s)$	$6.0 \cdot 10^7$	5000
2 $O_2(s) \rightarrow O_2 + s$	$2,3 \cdot 10^{12}$	38,000
3 $O_2(s) + s \rightarrow 2O(s)$	$2.3 \cdot 10^{23}$	25,000
4 $2O(s) \rightarrow O_2(s) + s$	$3.3 \cdot 10^{23}$	33,000
5 $CH_4 + O(s) \rightarrow CH_3\cdot + OH(s)$	$3.0 \cdot 10^8$	8840
6 $C_2H_6 + O(s) \rightarrow C_2H_5\cdot + OH(s)$	$8.7 \cdot 10^9$	3000
7 $CO + O(s) \rightarrow CO_2 + s$	$8.3 \cdot 10^8$	0
10 $C_2H_4 + O(s) \rightarrow C_2H_3\cdot + OH(s)$	$1.1 \cdot 10^{10}$	3000
13 $2OH(s) \rightarrow O(s) + H_2O + s$	$3.0 \cdot 10^{23}$	2400
24 $CH_4 + s \rightarrow CH_3\cdot + H(s)$	$8.5 \cdot 10^7$	9850
25 $C_2H_6 + s \rightarrow C_2H_5\cdot + H(s)$	$9.8 \cdot 10^7$	5000
26 $C_2H_4 + s \rightarrow C_2H_3\cdot + H(s)$	$1.9 \cdot 10^7$	5000
27 $H\cdot + s \rightarrow H(s)$	$9.6 \cdot 10^{12}$	0
28 $OH(s) + H(s) \rightarrow H_2O + 2s$	$1.0 \cdot 10^{24}$	0
29 $H(s) + H(s) \rightarrow H_2 + 2s$	$4.0 \cdot 10^{23}$	0
30 $H_2 + 2s \rightarrow 2H(s)$	$6.1 \cdot 10^{16}$	0
31 $H_2 + O(s) \rightarrow OH(s) + H\cdot$	$2.0 \cdot 10^8$	0

to 2. The simulation very well reproduces the conversion of CH<sub>4</sub> and the production of the most important products.

#### 4.2. Partial oxidation of methane

Among the proposed methods for the production of hydrogen, the partial oxidation of methane has many advantages: the reaction is exothermic and it may be carried out in autothermal conditions. This reaction produces syngas:  $CH_4 + \frac{1}{2} O_2 = CO + 2 H_2$

The reaction was studied at various temperatures between 973 K and 1123 K over La<sub>2</sub>O<sub>3</sub> catalyst. Like for HOM, the ratio CH<sub>4</sub>/O<sub>2</sub> was 2. The concentration of sites over the surface L was unknown. So we used an average value of  $L = 910^{-11}$  mol.cm<sup>-2</sup> as the starting point. L was thus considered as an adjustable parameter and the value used after

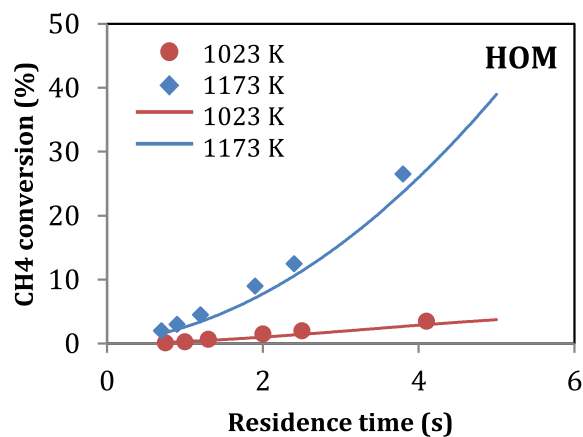


Fig. 4. Conversion of CH<sub>4</sub> versus residence time. Comparison between experiment (symbol) and simulation (line).

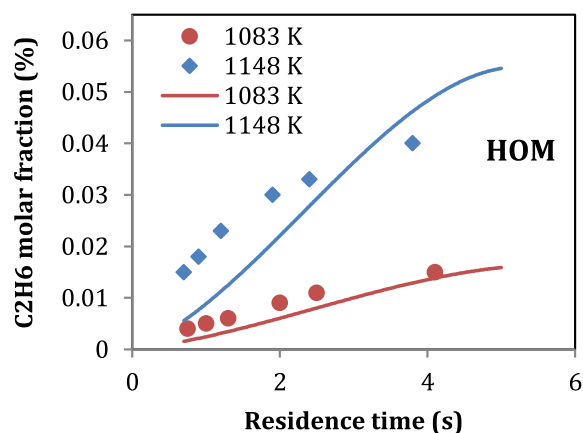


Fig. 5. Molar fraction of C<sub>2</sub>H<sub>6</sub> versus residence time. Comparison between experiment (symbol) and simulation (line).

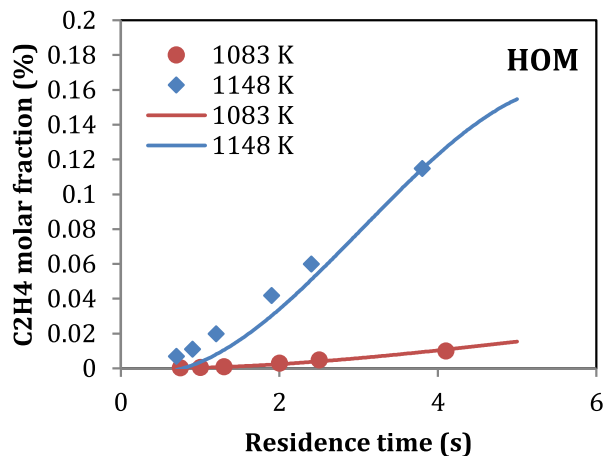


Fig. 6. Molar fraction of C<sub>2</sub>H<sub>4</sub> versus residence time. Comparison between experiment (symbol) and simulation (line).

adjustment was finally:

$L = 2.810^{-11}$  mol.cm<sup>-2</sup>. Figs. 10–15 show the variation of the molar fraction of CH<sub>4</sub>, C<sub>2</sub>H<sub>4</sub>, C<sub>2</sub>H<sub>6</sub>, CO, CO<sub>2</sub> and H<sub>2</sub> according to the residence time at two temperatures. A good agreement between the experimental and theoretical results can be observed.

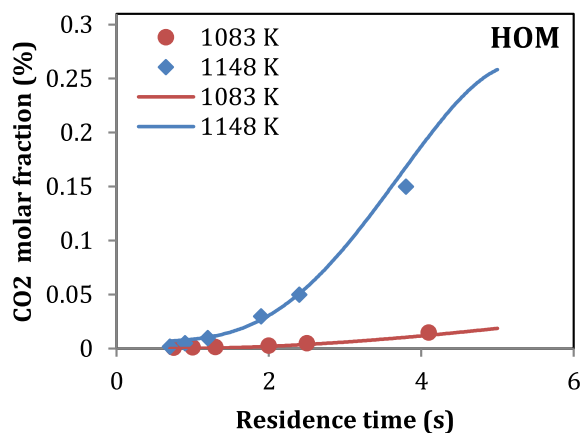


Fig. 7. Molar fraction of CO<sub>2</sub> versus residence time. Comparison between experiment (symbol) and simulation (line).

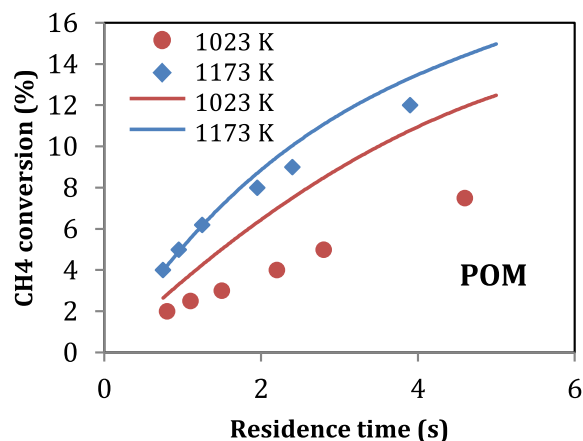


Fig. 10. Conversion of CH<sub>4</sub> versus residence time. Comparison between experiment (symbol) and simulation (line).

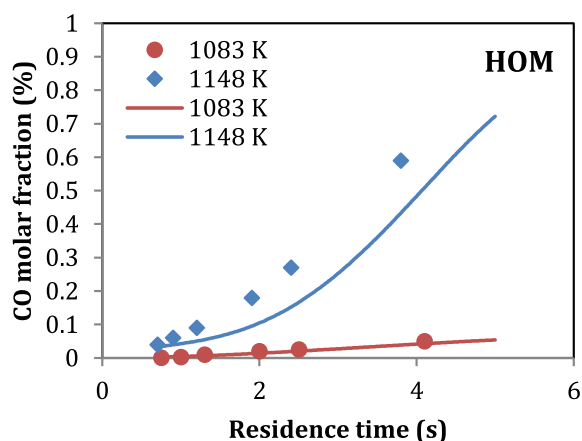


Fig. 8. Molar fraction of CO versus residence time. Comparison between experiment (symbol) and simulation (line).

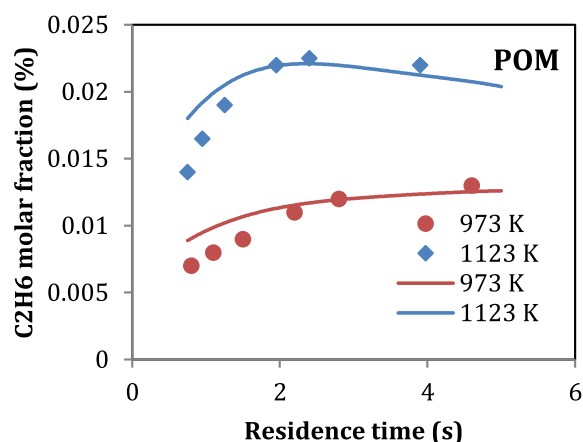


Fig. 11. Molar fraction of C<sub>2</sub>H<sub>6</sub> versus residence time. Comparison between experiment (symbol) and simulation (line).

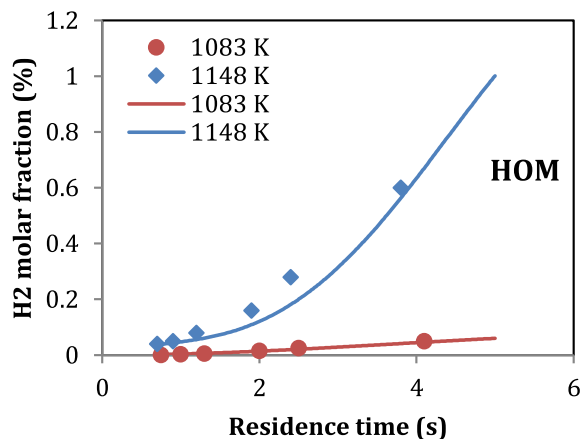


Fig. 9. Molar fraction of H<sub>2</sub> versus residence time. Comparison between experiment (symbol) and simulation (line).

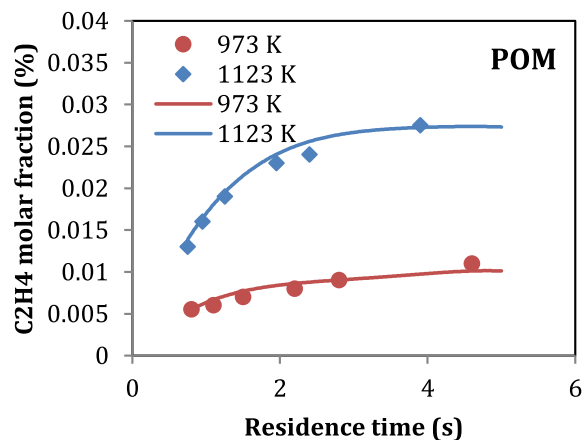
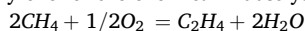


Fig. 12. Molar fraction of C<sub>2</sub>H<sub>4</sub> versus residence time. Comparison between experiment (symbol) and simulation (line).

#### 4.3. Oxidative coupling of methane

The reaction of oxidative coupling of methane has been investigated in a large number of laboratories because its development should have led to a direct process to obtain more valuable hydrocarbons such as ethylene for the chemical industry:



This reaction was studied between 1023 K and 1173 K over La<sub>2</sub>O<sub>3</sub> catalyst with a CH<sub>4</sub>/O<sub>2</sub> ratio of 5. Like for POM, the concentration of sites over the surface was  $L = 910^{-11} \text{ mol.cm}^{-2}$  as the starting point and the value used after adjustment was  $L = 510^{-11} \text{ mol.cm}^{-2}$ . Figs. 16–20 shows the molar fraction of CH<sub>4</sub>, C<sub>2</sub>H<sub>4</sub>, C<sub>2</sub>H<sub>6</sub>, CO and CO<sub>2</sub> according to the residence time. Although the kinetic parameters were only slightly

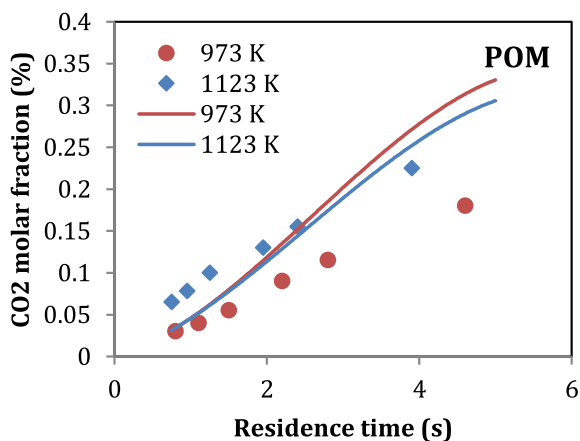


Fig. 13. Molar fraction of CO<sub>2</sub> versus residence time. Comparison between experiment (symbol) and simulation (line).

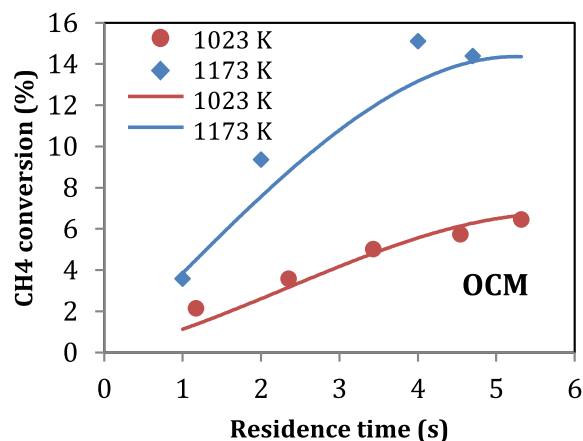


Fig. 16. Conversion of CH<sub>4</sub> versus residence time. Comparison between experiment (symbol) and simulation (line).

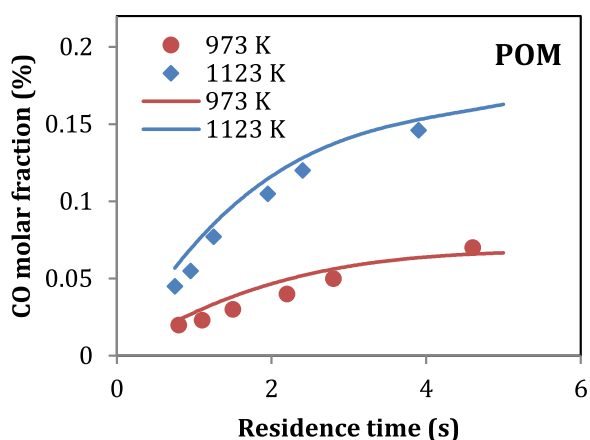


Fig. 14. Molar fraction of CO versus residence time. Comparison between experiment (symbol) and simulation (line).

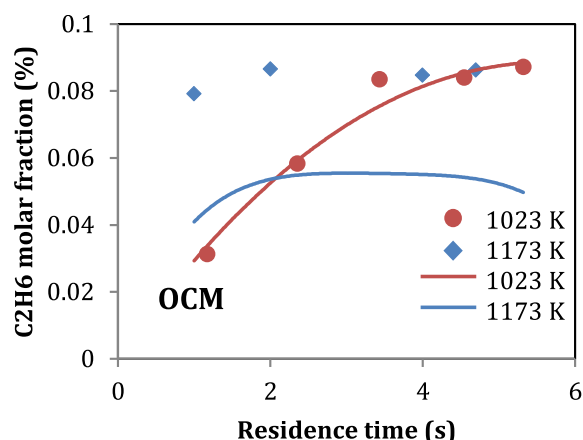


Fig. 17. Molar fraction of C<sub>2</sub>H<sub>6</sub> versus residence time. Comparison between experiment (symbol) and simulation (line).

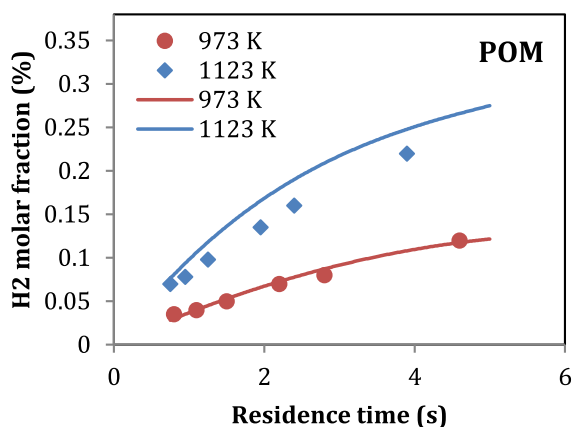


Fig. 15. Molar fraction of H<sub>2</sub> versus residence time. Comparison between experiment (symbol) and simulation (line).

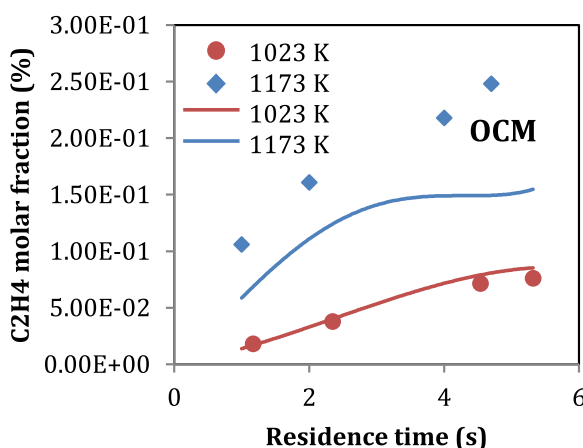


Fig. 18. Molar fraction of C<sub>2</sub>H<sub>4</sub> versus residence time. Comparison between experiment (symbol) and simulation (line).

modified the agreement between the theoretical curves and the experimental points was correct. Therefore the hetero-homogeneous mechanism was validated in the experimental conditions.

#### 4.4. Comparison of the three reactions

A simplification of the general mechanism can be represented

according to Fig. 21. The mechanism of oxidation of methane comprises two distinct reaction pathways: an oxidative route and a non-oxidative route.

The initiation of the oxidation of methane forms CH<sub>3</sub>· radicals (reaction 1). In the case of HOM, the activation occurs by reaction between CH<sub>4</sub> and a gas phase radical while in OCM and POM the initiation takes

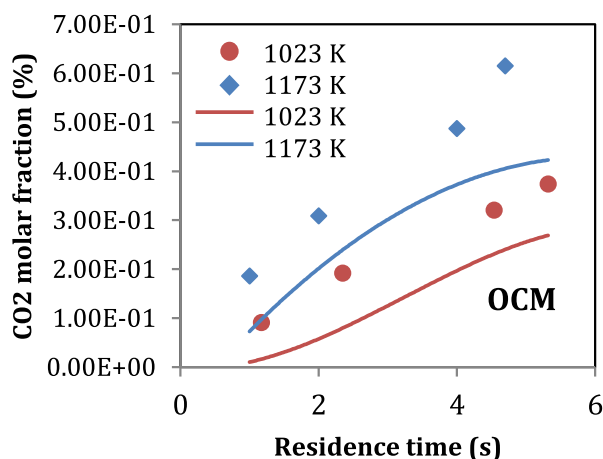


Fig. 19. Molar fraction of CO<sub>2</sub> versus residence time. Comparison between experiment (symbol) and simulation (line).

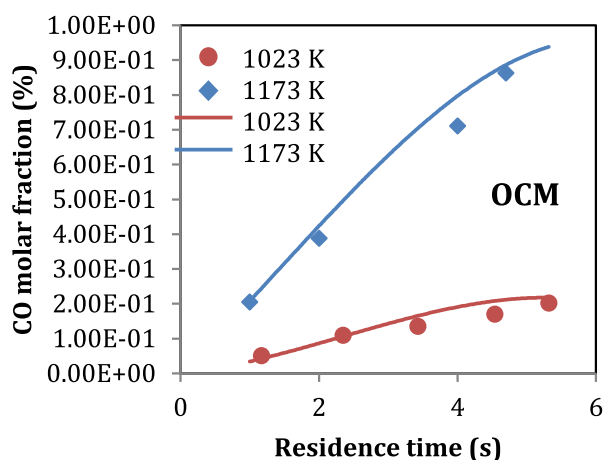


Fig. 20. Molar fraction of CO versus residence time. Comparison between experiment (symbol) and simulation (line).

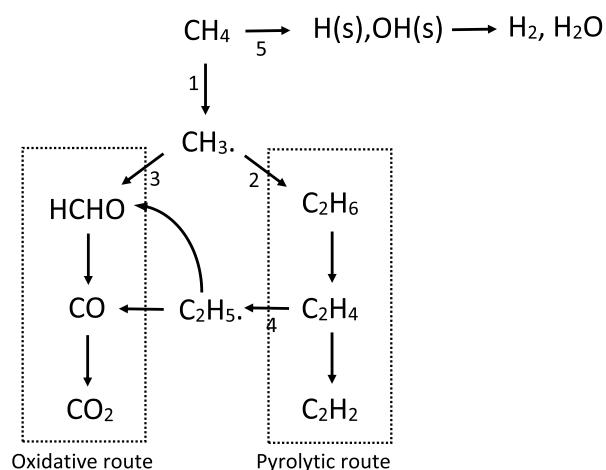
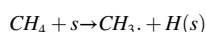
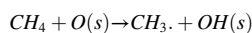


Fig. 21. Schematic representation of the mechanism.

place mainly on the catalyst by reactions involving surface species.



Heterogeneous initiations represent 80% of the methane activation in the case of POM and 100% in the case of OCM. The main effect of the catalyst is the generation of free radicals.

Then, the CH<sub>3</sub>· radicals can react according to the pyrolytic route (reaction 2) to form hydrocarbons or the oxidative route (reaction 3) to form oxygenated compounds. The pyrolytic route and therefore the formation of hydrocarbons is favored when the concentration of oxygen is low, which is the case for OCM. When the conversion is high, an oxidative step appears (reaction 4). This step decreases the concentration of C<sub>2</sub>H<sub>4</sub> and may explain why the yield of hydrocarbons in OCM does not exceed 22% to 27% for all catalysts tested, like reported by numerous authors.

In POM and HOM, the oxygen concentration favors the oxidative pathway. However, lanthanum oxide is an excellent generator of free radical. Thus, in POM, the catalyst more easily generates radicals by reactions between CH<sub>4</sub> and surface species and therefore accelerates the reaction. In addition, a new source of H<sub>2</sub> formed by heterogeneous reactions (reaction 5) appears on lanthanum oxide, which increases the yield of H<sub>2</sub> in POM.

## 5. Conclusion

The study of catalytic oxidations of methane has met with renewed interest in the past 10 years due to the discovery of new natural gas fields and the rising price of oil. These catalytic reactions are carried out at high temperature and thus comport a homogeneous and heterogeneous part, which make their mechanism more complex. This reaction mechanism is essential for the development of industrial processes. We have therefore developed a reaction mechanism that allows representing, at the same time, three methane oxidation reactions: homogeneous oxidation, partial oxidation and oxidative coupling. The homogeneous mechanism may be found in the literature or determined from an automatic generator of mechanism. The heterogeneous mechanism was written following the Eley-Rideal and Langmuir-Hinshelwood formalisms. The pre-exponential factor was determined by methods derived from Benson's technics whereas the activation energy was chosen, in a first time, by analogy with gas phase reactions. Finally, the mechanism used for the simulation give good results although the values of the rate constants were only slightly modified. Thanks to the sensitivity analysis, the heterogeneous mechanism has been simplified and contains only 17 elementary reactions.

## CRedit authorship contribution statement

**Yves Simon:** Conceptualization, Methodology, Formal analysis, Writing - review & editing. **Paul-Marie Marquaire:** Supervision, Funding acquisition.

## Declaration of Competing Interest

The authors declare that they have no known competing financial interests or personal relationships that could have appeared to influence the work reported in this paper.

## References

- [1] BP statistical review of world energy 2020.
- [2] Keller GE, Bhasin MM. Synthesis of Ethylene via Oxidative Coupling of Methane I. Determination of Active Catalysts. *J Catal* 1982;73:9–19.
- [3] Choudhary VR, Mulla SAR, Uphade BS. Oxidative coupling of methane over alkaline earth oxides deposited on commercial support pre-coated with rare earth oxides. *Fuel* 1999;78(4):427–37.
- [4] Rostrup-Nielsen JR, Christiansen LJ, Bak Hansen JH. Activity of steam reforming catalysts: role and assessment. *Appl Catal* 1988;43(2):287.
- [5] Rostrup-Nielsen JR, Sehested J, Nørskov JK. Hydrogen and Synthesis Gas by Steam and CO<sub>2</sub> Reforming. *Adv Catal* 2002;47:65.
- [6] Corbo P, Migliardini F. Hydrogen production by catalytic partial oxidation of methane and propane on Ni and Pt catalysts. *Int J Hydrogen Energy* 2007;32(1): 55–66.

- [7] Requies J, Barrio VL, Cambra JF, Güemez MB, Arias PL, La Parola V, et al. Effect of redox additives over Ni/Al<sub>2</sub>O<sub>3</sub> catalysts on syngas production via methane catalytic partial oxidation. *Fuel* 2008;87(15-16):3223–31.
- [8] Subramanian R, Panuccio GJ, Krummenacher JJ, Lee IC, Schmidt LD. Catalytic partial oxidation of higher hydrocarbons: reactivities and selectivities of mixtures. *Chem Eng Sci* 2004;59:5501.
- [9] Bistolfi M, Fornasari G, Molinari M, Palmery S, Dente M, Ranzi E. Kinetic Model for methane oxidative coupling reactors. *Chem Eng Sci* 1992;47:2647.
- [10] Driscoll DJ, Lunsford JH. Gas-phase radical formation during the reaction of methane, ethane, ethylene and propylene over selected oxide catalysts. *J Phys Chem* 1985;89:4415.
- [11] Driscoll DJ, Martir W, Wang J, Lunsford JH. Formation of gas phase methyl radicals over MgO. *J Am Soc* 1985;107:58.
- [12] Sinev MY. Kinetic modeling of heterogeneous-homogeneous radical processes of the partial oxidation of low paraffins. *Catal Today* 1995;24(3):389–93.
- [13] Baerns M, Buyevskaya OV, Mleczko L, Wolf D. Catalytic partial oxidation of methane to synthesis gas - catalysis and reaction engineering. *Stud Surf Sci Catal* 1997;107.
- [14] Deutschmann O, Schmidt LD. Modeling the partial oxidation of methane in a short-contact-time reactor. *AIChE J* 1998;44:2465.
- [15] Goralski CT, O'Connor RP, Schmidt LD. Modeling homogeneous and heterogeneous chemistry in the production of syngas from methane. *Chem Eng Sci* 2000;55:1357.
- [16] Fleys M, Simon Y, Marquaire PM. Discussion on the oxidative and the pyrolysis routes of the CH<sub>3</sub> radicals in the partial oxidation of methane over La<sub>2</sub>O<sub>3</sub>. *J Anal Appl Pyroly* 2007;79:259.
- [17] Thybaut JW, Sun J, Olivier L, Van Veen AC, Mirodatos C, Marin GB. Catalyst design based on microkinetic models: oxidative coupling of methane. *Catal Today* 2011; 159(1):29–36.
- [18] Hickman DA, Schmidt LD. Production of syngas by direct catalytic oxidation of methane. *Science* 1993;259(5093):343–6.
- [19] Vlachos DG. Homogeneous-heterogeneous oxidation reactions over platinum and inert surfaces. *Chem Eng Sci* 1996;51(10):2429–38.
- [20] Fleys M, Simon Y, Marquaire PM. Detailed kinetic study of the partial oxidation of methane over La<sub>2</sub>O<sub>3</sub> catalyst. Part 2: mechanism. *Ind Eng Chem Res* 2007;46: 1069–78.
- [21] Fleys M, Shan W, Simon Y, Marquaire PM. Detailed kinetic study of the partial oxidation of methane over La<sub>2</sub>O<sub>3</sub> catalyst. Part 1: Experimental results. *Ind Eng Chem Res* 2007;46:1063.
- [22] Fleys M, Simon Y, Swierczynski D, Kiennemann A, Marquaire P-M. Investigation of the reaction of partial oxidation of methane over Ni/La<sub>2</sub>O<sub>3</sub> catalyst. *Energy Fuels* 2006;20(6):2321–9.
- [23] Simon Y, Baronnet F, Marquaire PM. Kinetic modeling of the oxidative coupling of methane. *Ind Eng Chem Res* 2007;46:1914–22.
- [24] Barbé P, Li Y, Marquaire P-M, Côme G-M, Baronnet F. Competition between the gas and surface reactions for the oxidative coupling of methane. 1. "Non-isothermal" results in catalytic jet-stirred reactor. *Catal Today* 1994;21(2-3):409–15.
- [25] Barbé P, Li YD, Marquaire PM, Côme GM, Baronnet F. A new "catalytic jet-stirred reactor" Application to the study of the oxidative coupling of methane. *Oxid Commun* 1996;19:173.
- [26] Hognon C, Simon Y, Marquaire PM, Courson C, Kienneman A. Hydrogen production by catalytic partial oxidation of propane over CeO<sub>2</sub>. *Chem Eng Sc* 2018; 181:46–57.
- [27] Warth V, Battin-Leclerc F, Fournet R, Glaude PA, Côme GM, Scacchi G. Computer based generation of reaction mechanisms for gas-phase oxidation. *Comput Chem* 2000;24:541.
- [28] McCarty JG. *Methane Conversion by Oxidative Processes*, Wolf EE, Ed. Van Nostrand Reinhold, 1992 New York.
- [29] Martin GA, Mirodatos C. Surface chemistry in the oxidative coupling of methane. *Fuel Process Technol* 1995;42:179.
- [30] Lacombe S, Durjanova Z, Mleczko L, Mirodatos C. Kinetic modelling of the oxidative coupling of methane over lanthanum oxide in connection with mechanistic studies. *Chem Eng Technol* 1995;42:216.
- [31] Couwenberg PM, Chen Q, Marin GB. Kinetics of a gas-phase chain reaction catalysed by a solid: The oxidative coupling of methane over Li/MgO-based catalysts. *Ind Eng Chem Res* 1996;35:3999.
- [32] Wolf D, Slinko M, Kurkina E, Baerns. Kinetic simulations of surface processes of the oxidative coupling of methane over a basic oxide catalyst. *Appl Catal A* 1998;166 (1):47–54.
- [33] Coulter K, Goodman DW. The role of carbon dioxide in the oxidative dimerization of methane over Li/MgO. *Catal Lett* 1993;20:169.
- [34] Shi C, Xu M, Rosynek MP, Lunsford JH. Origin of kinetic isotope effects during the oxidative coupling of methane over a lithium (1+)/magnesia catalyst. *J Phys Chem* 1993;97:216.
- [35] Sinev MY, Fattakhova ZT, Lomonosov VI, Gordienko AY. Kinetics of oxidative coupling of methane: Bridging the gap between comprehension and description. *J Nat Gas Chem* 2009;18:273–87.
- [36] Karakaya C, Zhu H, Loebick C, Weissman JG, Kee RJ. A detailed reaction mechanism for oxidative coupling of methane over Mn/Na<sub>2</sub>WO<sub>4</sub>/SiO<sub>2</sub> catalyst for non-isothermal conditions. *Catal Today* 2018;312:10.
- [37] Beck B, Fleischer V, Arndt S, Hevia MG, Urakawa A, Hugo P, et al. *Catal Today* 2014;228:212.
- [38] Yang T, Feng L, Shen S. Oxygen species on the surface of La<sub>2</sub>O<sub>3</sub>/CaO and its role in the oxidative coupling of methane. *J Catal* 1994;145:384.
- [39] Hutchings GJ, Woodhouse JR, Scurrell MS. Partial oxidation of methane over oxide catalysts. Comments on the reaction mechanism, *J. Chem. Soc. Faraday Trans* 1989;85:2507.
- [40] Lacombe S, Geantet C, Mirodatos C. Oxidative coupling of methane over lanthana catalysts. I. Identification and role of specific active sites. *J Catal* 1994;151:439.
- [41] Huang S-J, Walters AB, Vannice MA. Adsorption and decomposition of NO on lanthanum oxide. *J Catal* 2000;192:29.
- [42] Gambo Y, Jalil AA, Triwahyono S, Abdulrasheed AA. Recent advances and future prospect in catalysts for oxidative coupling of methane to ethylene : A review. *J Ind Eng Chem* 2018;59:218–29.
- [43] Zerkle DK, Allendorf MD, Wolf M, Deutschmann O. Understanding homogeneous and heterogeneous contributions to the platinum-catalyzed partial oxidation of ethane in a short-contact-time reactor. *J Catal* 2000;196:18–39.
- [44] Sinev MY. Free radicals in catalytic oxidation of light alkanes: kinetic and thermochemical aspects. *J Catal* 2003;216(1-2):468–76.
- [45] Sun J, Thybaut J, Marin G. Microkinetics of methane oxidative coupling. *Catal Today* 2008;137(1):90–102.
- [46] Benson SW. *Thermochemical kinetics : methods for the estimation of thermochemical data and rate parameters*. New York: J. Wiley & sons; 1976.
- [47] Glarborg P, Kee RJ, Grear JF, Miller JA. PSR: a Fortran program for modeling well-stirred reactors. *Sandia Report* 1990;SAND86-8209-UC-4.
- [48] Coltrin ME, Kee RJ, Rupley FM, Surface Chemkin (v 4.0): a Fortran package for 16 analyzing heterogeneous chemical kinetics at a solid surface - gas phase interface, *Sandia Report*, SAND90-8003C – UC-706, 1991.
- [49] Toops TJ, Walters AB, Vannice MA. The effect of CO<sub>2</sub> and H<sub>2</sub>O on the kinetics of NO reduction by CH<sub>4</sub> over La<sub>2</sub>O<sub>3</sub>/γ-Al<sub>2</sub>O<sub>3</sub> catalyst. *J Catal* 2003;214:292–307.
- [50] Baulch DL, Cobos CJ, Cox RA, Esser C, Frank P, Just Th, et al. Evaluated kinetic data for combustion modelling. *J Phys Chem Ref Data* 1992;21(3):411–734.
- [51] Tsang W, Hampson RF. Chemical kinetic data base for combustion chemistry. Part I. methane and related compounds. *J Phys Chem Ref Data* 1986;15(3):1087–279.
- [52] Ranzi E, Sogaro A, Gaffuri P, Pennati G, Faravelli T. A wide range modelling study of methane oxidation. *Comb Sci and Technol* 1994;96:279.
- [53] Cavanagh J, Cox RA, Olson G. Computer modeling of cool flames and ignition of acetaldehyde. *Comb Flame* 1990;82(1):15–39.
- [54] Schulz G, Klotz H-D, Spangenberg H-J. Reaktionsmodell zur bruttonetkinetik der pyrolyse von methan im stosswellenrohr bei temperaturen von 1800 K bis 2500 K. *Z Chem* 1985;25:88.
- [55] Knyazev VD, Bencsura A, Stoliarov SI, Slagle IR. Kinetics of the C<sub>2</sub>H<sub>3</sub> + H<sub>2</sub> = H + C<sub>2</sub>H<sub>4</sub> and CH<sub>3</sub> + H<sub>2</sub> = H + CH<sub>4</sub> reactions. *J Phys Chem* 1996;100:11346.
- [56] Zhang HX, Ahonkhai SI, Back MH. Rate constants for abstraction of hydrogen from benzene, toluene, and cyclopentane by methyl and ethyl radicals over the temperature range 650–770 K. *Can J Chem* 1989;67:1541.
- [57] Benson SW. *Oxygen Initiated Combustion: Thermochemistry and Kinetics of Unsaturated Hydrocarbons*. *Int J Chem Kin* 1996;28(9):665–72.
- [58] Mahmud K, Marshall P, Fontijn A. A high-temperature photochemistry kinetics study of the reactions of O Atoms With Acetylene From 290 to 1510 K. *J Phys Chem* 1987;91:1568.
- [59] Glarborg P, Miller JA, Kee RJ. Kinetic modeling and sensitivity analysis of nitrogen oxide formation in well-stirred reactors. *Comb Flame* 1986;65(2):177–202.
- [60] Warth V, Stef N, Glaude PA, Battin-Leclerc F, Scacchi G, Côme G-M. Computed aided design of gas-phase oxidation mechanisms: Application to the modelling of normal-butane oxidation. *Comb Flame* 1998;114:81–102.